

Phase Estimation of a Single Quasi-Periodic Signal

Yasushi Makihara, Muhammad Rasyid Aqmar, Ngo Thanh Trung, Hajime Nagahara, *Member, IEEE*,
Ryusuke Sagawa, *Member, IEEE*, Yasuhiro Mukaigawa, *Member, IEEE*, and Yasushi Yagi, *Member, IEEE*

Abstract—We propose a method for phase estimation of a single non-parametric quasi-periodic signal. Assuming signal intensities should be equal among samples of the same phase, such corresponding samples are obtained by self-dynamic time warping between a quasi-periodic signal and a signal with multiple-period shifts applied. A phase sequence is then estimated in a sub-sampling order using an optimization framework incorporating 1) a data term derived from the correspondences and 2) a smoothness term of the local phase evolution under 3) a monotonic-increasing constraint on the phase. Such a phase estimation is, however, ill-posed because of combination ambiguity between the phase evolution and the normalized periodic signal, and hence can result in a biased solution. Therefore, we introduce into the optimization framework 4) a bias correction term, which imposes zero-bias from the linear phase evolution. Analysis of the quasi-periodic signals from both simulated and real data indicate the effectiveness and also potential applications of the proposed method.

Index Terms—Phase, quasi-periodic signal, dynamic time warping.

I. INTRODUCTION

PERIODIC signal analysis has been widely applied in the signal processing field as well as in the fields of image processing, computer vision, and pattern recognition. Fundamentally, periodic signals play quite an important role in many applications ranging from data transmission via a radio carrier wave [1], [2] in electronic communications to periodic motion detection from video [3], [4], periodic action recognition [5] (e.g., walking and running), and person authentication or identification from periodic action (e.g., gait-based person identification [6]) in the computer vision and pattern recognition fields.

Manuscript received January 04, 2013; revised July 11, 2013 and December 12, 2013; accepted January 27, 2014. Date of publication February 13, 2014; date of current version March 19, 2014. The associate editor coordinating the review of this manuscript and approving it for publication was Prof. Emmanuel Candes. This work was supported by JSPS Grant-in-Aid for Scientific Research(S) 21220003 and Young Scientists (A) 23680017, and the JST CREST “Behavior Understanding based on Intension-Gait Model” project.

Y. Makihara, M. R. Aqmar, N. T. Trung, Y. Mukaigawa, and Y. Yagi are with the Institute of Scientific and Industrial Research, Osaka University, Osaka, 567-0047, Japan (website: <http://www.am.sanken.osaka-u.ac.jp/index.html>).

H. Nagahara is with the Faculty of Information Science and Electrical Engineering, Kyushu University, Fukuoka 812-8581, Japan (e-mail: nagahara@ait.kyushu-u.ac.jp).

R. Sagawa is with Intelligent Systems Research Institute, National Institute of Advanced Industrial Science and Technology, Tsukuba 305-8568, Japan.

This paper has supplementary downloadable multimedia material available at <http://ieeexplore.ieee.org> provided by the authors. This includes a video file, which shows the application example of phase estimation and normalization by the proposed method to synchronize the phase between walking and running. This material is 4.4 MB in size.

Color versions of one or more of the figures in this paper are available online at <http://ieeexplore.ieee.org>.

Digital Object Identifier 10.1109/TSP.2014.2306174

Such periodic signals are often modulated in amplitude, frequency, and/or phase by design or by chance. We refer such a modulated version of a periodic signal in terms of frequency, phase, and/or amplitude, to a *quasi-periodic signal*. Typical examples of intentional modulation are amplitude modulation (AM) and frequency modulation (FM) [1] used in radio broadcasts, and phase modulation (PM) [2] used in radio control, where a carrier wave with known parameters is given as a reference and the modulation is estimated from the carrier wave.

In contrast, accidental modulation is induced by a fluctuation in the sampling interval (e.g., a network camera with limited communication bandwidth) or the periodic signal source itself (e.g., fluctuations in human walking patterns). Estimating phases from such phase-modulated quasi-periodic signals is quite an important function for many applications. For example, temporal interpolation of a video with constant phase evolution needs the correct phase information for each key frame. Moreover, temporal super resolution of a periodic image sequence [7] needs accurate phase registration data among multiple periods with sub-sampling order displacement of phase, in the same way that spatial super resolution needs image registration data with sub-pixel order displacement [8]. Phase registration data are also essential to reconstruct a manifold parameterized by phase in periodic action analysis [9] and recognition and accurate period segmentation for periodic signal matching [10]. In cases where a reference periodic signal is available, dynamic time warping (DTW) [11] (more specifically, continuous dynamic programming (DP) [12] in the periodic signal case) is a powerful tool for matching two sequences with non-linear time warping, in the sense that matching results give phase registration data. A reference signal is, however, usually unavailable in the above applications.

This paper tackles the challenging problem of phase estimation from a *single quasi-periodic signal*. Given that signal intensities should be equal among samples of the same phase, such related samples are obtained by self DTW between a quasi-periodic signal and a signal with multiple-period shifts applied. A phase sequence is then estimated in a sub-sampling order within an optimization framework including (1) a data term derived from the correspondences and (2) a smoothness term of the local phase evolution under (3) a monotonic increasing constraint on the phase.

Whereas the above optimization framework provides satisfactory results in terms of phase registration or period segmentation, it sometimes fails in terms of *phase estimation* due to phase bias within a period. It has been reported that there is a combination ambiguity of the phase evolution function¹ and

¹A phase evolution function maps time to phase (non-dimensional time).

normalized periodic signal in the phase domain² (see Fig. 3); in other words, different combinations of phase evolution functions and normalized periodic signals in the phase domain possibly produce the same quasi-periodic signal [13]. As a result, a biased phase evolution function and a phase-biased normalized periodic signal can be reconstructed from a given quasi-periodic signal.

Therefore, as an extension from our previous work [13], we further introduce into the optimization framework (4) a bias-correction term which imposes zero-bias from the linear phase evolution, which is essential to overcome the combination ambiguity problem. This enables us to construct an unbiased phase evolution function and normalized periodic signal and to improve the accuracy of the phase estimation.

II. RELATED WORK

Parametric Representation: A periodic signal is usually represented by a periodic function parameterized by amplitude, frequency, and phase, and is often observed together with additive noise. This parametric expression is widely used in the context of periodic signal reconstruction [14] and detection [15], enhancement of a specific frequency [16], estimation of frequency [17], estimation of amplitude [18], estimation of phase [19], [20], phase synchrony [21], and decomposition of multiple periodic signals [22]–[24].

The common technique vital in these approaches is parameter estimation; henceforth, non-parametric periodic signals are beyond the scope of these studies.

Non-Parametric Representation: Non-parametric approach does not assume the model is fixed by some parameters (e.g., frequency, phase, or amplitude) and thus, require less assumptions on the model to estimate the parameters of any periodic signal. In fact, our work proposed in this paper falls into this category. As closely related literature to our work, Daubechies *et al.* [25] proposed a robust signal decomposition method based on time-frequency plane construction by Wavelet transform so called synchrosqueezed wavelet transform (SST). This method is able to deal with general AM and FM signals. The SST decomposes the signal into multiple components of amplitude and frequency, and it is able to reconstruct the original signal by those components with high accuracy. Some of the applications of the SST can be found on Chen *et al.* [26] and Wu [27], which estimates an instantaneous frequency (an inverse of the instantaneous period) from a single quasi-periodic signal. The phase is then estimated via components reconstruction and phase unwrapping. This method requires quite large number of frequency components for accurate representation.

Seitz and Dyer [28] proposed a robust method to trace an instantaneous period³ in a quasi-periodic signal and applied it to irregularity detection. The phase then can be estimated via frame-by-frame recurrence formula based on the instantaneous frequency or period. However, this phase estimation method often suffers from accumulation errors.

²A normalized periodic signal is a periodic function of a phase. The normalized periodic signal is converted to an original quasi-periodic signal via the inverse function of the phase evolution function.

³A instantaneous period $P_Q(t)$ at time t means a period just at the moment of time t and it may change across time.

Linear Time Warping: Linear time warping is conventionally used in periodic action recognition such as gait recognition [29]–[31]. Periods are usually first detected by an interval of signal peaks [6], maximum entropy spectrum estimation [32], or maximum normalized autocorrelation [33]. The signals are then linearly stretched/shrunk so that the periods of two signals match. Naturally, these methods cannot deal with non-linear time warping within a period.

Non-Linear Time Warping: DTW [11] was introduced to match time-varying signals in the field of speech recognition [34], [35]. DTW has been also widely used for elastic matching of two sequences in the field of action recognition [36] and gait recognition [37]. The hidden Markov model (HMM), a probabilistic framework version of the DTW, is one of the standard approaches for automatic speech recognition [38], [39]. The HMM is also used in phase state estimation in walker motion extraction [40], gait silhouette refinement [41], [42], and gait recognition [43], [44]. The HMM, however, needs sufficient training sequences and hence, cannot be applied directly to phase estimation from a single sequence. Moreover, the number of states should be sufficiently large to realize a sub-sampling order phase estimation and this leads to an explosive increase in the number of training samples required.

Recently, Li and Chellappa [45] proposed a robust alignment method applied not only in time domain, but also in 2D spatial domain using spatio-temporal non-linear manifold. This method solves the spatial misalignment due to deforming shape of spatial signal as well as the temporal misalignment due to different rate between two signals. Another method based on spatial and temporal periodic normalization was proposed by Polana and Nelson [46] for motion detection and recognition. These methods, however, require a template sequence for alignment and hence cannot be used for the main purpose of this paper; phase estimation only from a single quasi-periodic signal.

Moreover, Makihara *et al.* [7] proposed a method of periodic temporal super resolution from a single quasi-periodic image sequence. While it can cope with a low frame-rate video, it imposes a strong assumption that exactly the same periodic images are observed among all the periods. Therefore, it does not work on the image sequences with view and speed transitions. Note that although the work [7] also involves phase estimation step in the framework and that the phase estimation is done using the reconstructed periodic image sequence as a reference signal, which falls into a family of DTW between two different signals (e.g., input and reference signals).

III. PROBLEM SETTING

First, the generation process of a quasi-periodic signal (Fig. 1) is introduced in this section. Given a multi-dimensional periodic signal $f(t)$ with period P that satisfies

$$f(t + jP) = f(t) \quad \forall j \in \mathbb{Z}, \quad (1)$$

where \mathbb{Z} is a set of natural number, a time normalized by period P is introduced as an absolute phase s and a relative phase \tilde{s} as

$$s = s_P(t) = \frac{1}{P}t \quad (2)$$

$$\tilde{s} = s - \lfloor s \rfloor, \quad (3)$$

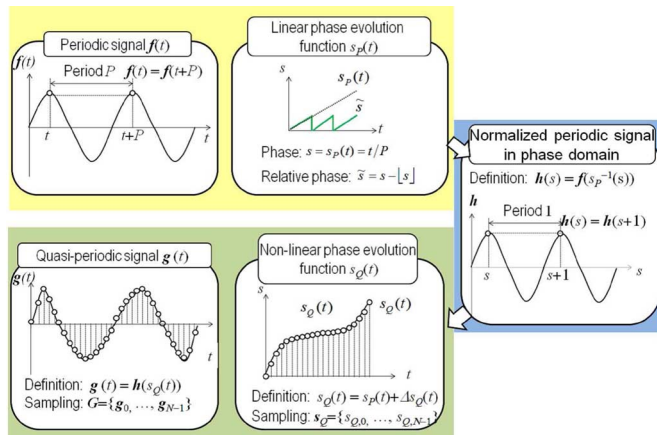


Fig. 1. Process of generating a quasi-periodic signal.

where $s_P(t)$ is a phase evolution function which maps time t to phase s , and $\lfloor \cdot \rfloor$ is the floor function. A periodic signal in the phase domain (later, we call this the normalized periodic signal) is subsequently introduced as

$$h(s) = f(s_P^{-1}(s)), \quad (4)$$

which satisfies

$$h(s + j) = h(s) = h(\bar{s}) \quad \forall s, \quad (5)$$

where $s_P^{-1}(s)$ is an inverse function of the phase evolution function $s_P(t)$ which maps phase s to time t . Note that $h(s + j)$ means a signal intensity with j periods shift and that it coincides with the original signal intensity $h(s)$.

Next, it is assumed that the phase evolution function $s_P(t)$ is modulated by fluctuations into $s_Q(t)$ and that the periodic signal $f(t)$ is converted to a quasi-periodic signal $g(t)$, which is subject to

$$g(t) = h(s_Q(t)) = f(s_P^{-1}(s_Q(t))). \quad (6)$$

Conversely, given the quasi-periodic signal $g(t)$ and its phase evolution function $s_Q(t)$, the normalized periodic signal is reconstructed as

$$h(s) = g(s_Q^{-1}(s)). \quad (7)$$

In addition, because the signal is usually sampled through observation, we redefine the above variables at sampling time t_i ($i = 0, \dots, N - 1$) with subscription i (e.g., $g_i = g(t_i)$). Therefore, our objective is to estimate a phase evolution sequence $S_Q = \{s_{Q,i}\}$ from a given quasi-periodic signal $G = \{g_i\}$. This is referred to as the *phase estimation* problem in this paper.

IV. PHASE ESTIMATION USING SELF DTW

A. Optimization Framework

In order to solve the phase estimation problem described in Section III, the phase evolution sequence S_Q is optimized by minimizing a certain objective function $D(S_Q)$ composed of

(1) a data term $D_d(S_Q)$ which establishes the relation between a phase and another phase with several periods shift, and (2) a smoothness (or regularization) term $D_s(S_Q)$ which makes the local phase evolution speed (the first-order differential of the phase evolution function) coincide with an instantaneous frequency under (3) a monotonic increasing constraint on the phase evolution function as

$$S_Q^* = \arg \min_{S_Q} D(S_Q) \quad (8)$$

$$D(S_Q) = D_d(S_Q) + \lambda_s D_s(S_Q) \quad (9)$$

$$D_d(S_Q) = \sum_j \sum_{[i,u] \in X^j} (s_{Q,u} - s_{Q,i} - j)^2 \quad (10)$$

$$D_s(S_Q) = \sum_{i=0}^{N-2} \left(s_{Q,i+1} - s_{Q,i} - \frac{1}{\hat{P}_{Q,i}} \right)^2 \quad (11)$$

$$\text{subject to } s_{Q,i+1} - s_{Q,i} \geq 0 \quad \forall i = 0, \dots, N - 2, \quad (12)$$

where X^j is a set of corresponding pairs of frames whose phase difference is j , which means j periods shift (call this a j -th period correspondence pair later), $\hat{P}_{Q,i}$ is an estimated instantaneous period at the i -th frame, whose inverse is equivalent to the instantaneous frequency at the i -th frame, and λ_s is the smoothness coefficient.

While the data term is derived from the signal intensity consistency at the same relative phase as described later in Subsection IV-C, the smoothness term is derived from the relationship between the phase and the frequency/period as follows. First, it is well known that the first-order differential of the phase evolution function $s_Q(t)$ coincide with the instantaneous frequency $F_Q(t)$ at time t , which is equivalent to the inverse of the instantaneous period $P_Q(t)$ at time t , as

$$\frac{ds_Q(t)}{dt} = F_Q(t) = \frac{1}{P_Q(t)}. \quad (13)$$

Note that the instantaneous period $P_Q(t)$ is equivalent to the constant period P in a completely periodic signal, which is obvious from (2). For a sampled version, (13) becomes

$$s_{Q,i+1} - s_{Q,i} = F_{Q,i} = \frac{1}{P_{Q,i}}, \quad (14)$$

where $F_{Q,i}$ and $P_{Q,i}$ are the instantaneous frequency and period at the i -th frame, respectively. We now notice that the smoothness term $D_s(S_Q)$ is defined as summation of the squared errors of (14).

Moreover, even if a constant phase shift \bar{s} is added to the phase sequence as $s'_{Q,i} = s_{Q,i} + \bar{s}$, the value of the objective function (9) as well as the constraints (12) are not affected at all, because all $s_{Q,i}$ are used in a pairwise subtraction form. Therefore, the following constraint (an initial condition) is added without loss of generality

$$s_{Q,0} = 0. \quad (15)$$

Finally, because the objective function $D(S_Q)$ is a quadratic form and the constraints of (12) and (15) are linear forms, the above optimization problem is efficiently solved by convex quadratic programming using the active set method, given a set

X^j of j -th period correspondence pair and the estimated instantaneous period sequence $P_Q = \{P_{Q,i}\}(i = 0, \dots, N - 1)$. We describe the ways how to estimate them in the following subsections.

B. Instantaneous Period Estimation by Short-Term Period Detection (STPD)

In this subsection, we describe the way how to estimate instantaneous period sequence P_Q . First, we assume that the domain $[P_{\min}, P_{\max}]$ of the instantaneous period $P_{Q,i}$ is given by prior knowledge. A short-term normalized autocorrelation (NAC) is then introduced as

$$C_i(P_{Q,i}) = \frac{\sum_{\tau \in I_i} g_\tau^T g_{\tau+P_{Q,i}}}{\sqrt{\sum_{\tau \in I_i} \|g_\tau\|^2} \sqrt{\sum_{\tau \in I_i} \|g_{\tau+P_{Q,i}}\|^2}} \quad (16)$$

$$I_i = \{\tau \in \mathbb{Z} | i - \alpha P_{\max} \leq \tau \leq i + \alpha P_{\max}\}, \quad (17)$$

where $C_i(P_{Q,i})$ is the NAC at the i -th frame for the instantaneous period $P_{Q,i}$ and α is a coefficient to control the size of the window function for the short-term mask.

One of possible solutions to this is to just adopt an argument maximizing the NAC in (16) as the instantaneous period frame-by-frame [13]. In such a solution, k -times instantaneous period ($k \in \mathbb{Z}$) can sometimes be estimated by mistake, when the k -times instantaneous period is included in the domain $[P_{\min}, P_{\max}]$. This is because the k -times instantaneous period can also be another instantaneous period and hence the NAC for the k -times instantaneous period can exceed that for the correct instantaneous period. Abrupt changes or *jump* of the instantaneous periods due to this mis-detection can cause a failure in the optimization step, and hence a sequence of the instantaneous periods should keep C0 smoothness.

Therefore, instead of maximizing the NAC frame-by-frame, the DP framework is employed to estimate a C0-continuous sequence of the instantaneous periods. Let's define the instantaneous period sequence as $P_Q = \{P_{Q,i}\}(i = 0, \dots, N - 1)$ and also define the cumulative NAC $C(P_Q)$ as

$$C(P_Q) = \sum_{i=0}^{N-1} C_i(P_{Q,i}). \quad (18)$$

In addition, the transition constraint on the instantaneous periods between adjacent frames, as well as the range constraint of the instantaneous period frame-by-frame, are imposed as

$$|P_{Q,i+1} - P_{Q,i}| \leq \delta \quad (19)$$

$$P_{\min} \leq P_{Q,i} \leq P_{\max}, \quad (20)$$

where δ is a tolerance of instantaneous period change between adjacent frames, which is set to sufficiently small number to keep the C0 smoothness of the instantaneous period sequence. An instantaneous period sequence P_Q is then computed in the DP framework so as to maximize the cumulative NAC in (18) in a recursive way by taking into consideration the constraints in (19) and (20). After the maximum cumulative NAC at the final frame ($N - 1$) is found, the optimal path is back-tracked, which actually corresponds to the estimated instantaneous period sequence \hat{P}_Q .

Once the C0-continuous instantaneous period sequence \hat{P}_Q is obtained, the first-order derivative $\frac{ds_Q(t)}{dt}$ of the phase evolution function is also C0 continuous from (13) and the phase evolution function $s_Q(t)$ itself is therefore C1 continuous.

C. Self DTW

In this subsection, we describe the way how to obtain a set X^j of the j -th period correspondence pairs.

We denote a j -th period correspondence pair as $x_i^j = [i, u_i^j]$ at first. Remembering that the difference of the absolute phases between the j -th period correspondence pair x_i^j is j , it is ideally subject to the following phase constraint

$$s_{Q,u_i^j} - s_{Q,i} = j. \quad (21)$$

In addition, according to (5) and (6), signals for the j -th period correspondence pair x_i^j is subject to the following signal consistency

$$g_{u_i^j} = g_i. \quad (22)$$

Hence, the phase constraint in (21) is exploited as the data term in the optimization step, and we try finding the j -th period correspondence pair x_i^j based on the signal consistency in (22). For this purpose, we exploit *self DTW*, which is a variant of the conventional DTW. While the conventional DTW finds the optimal correspondence between two different signals (e.g., query and reference signals), the self DTW finds the optimal correspondence between a quasi-periodic signal and a period-shifted version of the same quasi-periodic signal. More specifically, a key procedure to the self DTW is to find the optimal paths as a set of the j -th period correspondence pair from a cost matrix whose (i, u) component is the signal difference at frames i and u . Although this process is similar to trace of the instantaneous period [28] to some extent, note that the self DTW finds multiple optimal paths ($j = 1, \dots$) based on the DP framework, the work [28] finds a single optimal path for $j = 1$ based on the snake fitting framework. The detailed procedures of the self DTW are described as below.

First, an initial estimate of the j -th period correspondence $\hat{x}_i^j = [i, \hat{u}_i^j]$ is obtained from the estimated instantaneous period $\hat{P}_{Q,i}$ in a recursive manner as

$$\hat{u}_i^0 = i, \hat{u}_i^j = \hat{u}_i^{j-1} + \hat{P}_{Q,\hat{u}_i^{j-1}} \quad (23)$$

Next, lower and upper bounds of the j -th period correspondence, namely, the boundaries of the so-called *corridor* of a DTW path search region, are set to

$$\hat{u}_{low,i}^j = \max\{\hat{u}_i^j - \beta \hat{P}_{Q,\hat{u}_i^j}, 0\} \quad (24)$$

$$\hat{u}_{up,i}^j = \min\{\hat{u}_i^j + \beta \hat{P}_{Q,\hat{u}_i^j}, N - 1\}, \quad (25)$$

where β is a coefficient to control the size of the corridor. Thus, a self DTW path search region is defined as $R^j = \{x = [i, u] | \hat{u}_{low,i}^j \leq u \leq \hat{u}_{up,i}^j \forall i \in [0, N]\}$, and subsequently the source and terminal regions are set to $R_S^j = \{x = [0, u] | x \in R^j\}$ and $R_T^j = \{x = [i, N - 1] | x \in R^j\}$, respectively, as illustrated in Fig. 2. Now, the correspondence

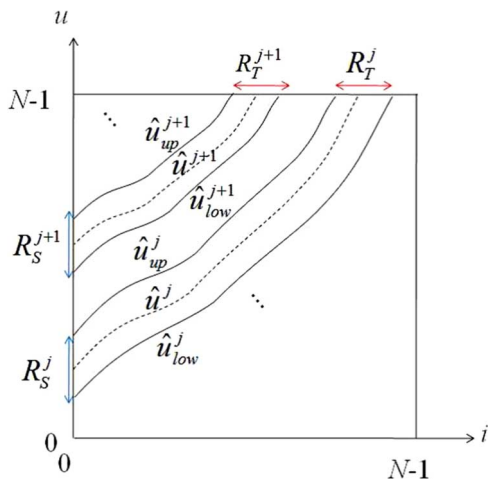


Fig. 2. Overview of Self DTW.

problem is decoded as continuous DP [12] in the search region R^j .

The formulation is given as follows. A cumulative cost $c(x)$ and a counter $n(x)$ are introduced and these are initialized for $x \in R_S^j$ as

$$c(x) = c_I(x), \quad n(x) = 1, \quad (26)$$

where $c_I(x)$ is a cost function for the signal intensity difference given as $c_I(x) = \|g_i - g_u\|$.

Next, a transition process is considered. We limit the previous state x_p to the current state x to $T^j(x) = \{[i-1, u-1], [i-2, u-1], [i-1, u-2]\} \cap R^j$ and define the optimal previous state to be the current state as $x_p^{j*}(x)$, which is given as

$$x_p^{j*}(x) = \arg \min_{x_p \in T^j(x)} \left\{ \frac{c(x_p)}{n(x_p)} + c_T(x, x_p) \right\}, \quad (27)$$

where the first and second terms on the right-hand side are, respectively, the counter-normalized previous cumulative cost and the transition cost function, given as $c_T(x, x_p) = \|x - x_p\|_{L_1}$. Then, the cumulative cost and the counter are updated as

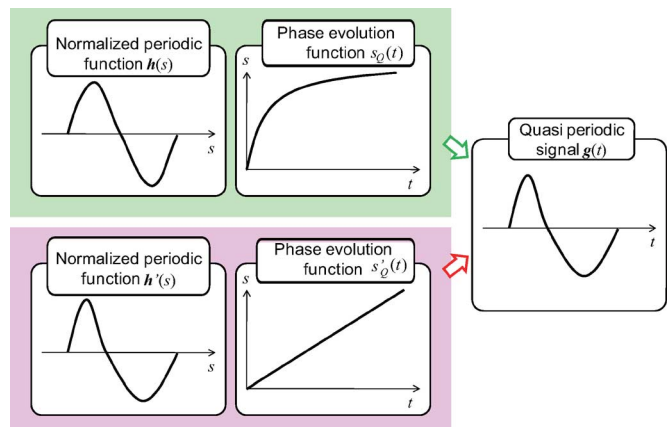
$$c(x) = c(x_p^{j*}(x)) + c_I(x) + c_T(x, x_p^{j*}(x)) \quad (28)$$

$$n(x) = n(x_p^{j*}(x)) + 1 \quad (29)$$

After the cost propagation of all the states in R^j , the optimal terminal state is

$$x_T^{j*} = \arg \min_{x \in R_T^j} \frac{c(x)}{n(x)}. \quad (30)$$

Subsequently, the terminal counter and the optimal terminal state are redefined, respectively, as $n^j = n(x_T^{j*})$ and $x_{n_j}^j = x_T^{j*}$ for convenience, and the optimal path is back-tracked as $x_i^{j*} = x_p^{j*}(x_{i+1}^{j*})$ for $i = n^j - 1, \dots, 1$. Finally, the optimal correspondence sequence is denoted as $X^j = \{x_i^{j*} | i = 1, \dots, n^j\}$.

Fig. 3. Combination ambiguity problem. Different combinations of phase evolution functions and normalized periodic signals potentially produce the same quasi-periodic signals $g(t)$.

V. GLOBAL OPTIMIZATION

A. Overview

In this section, we propose an improved version of phase estimation method. The estimation method by (8) in the previous section sometimes results in a biased phase sequence caused by a combination ambiguity problem of the phase evolution function and the normalized periodic signal as reported in [13]. We therefore incorporate a bias correction framework into the objective function for phase estimation. The details are explained in the following subsections.

B. Combination Ambiguity

In this subsection, we show an example of the combination ambiguity and also point out its problematic aspects.

Let's assume that a quasi-periodic signal $g(t)$ is derived from a combination of a phase evolution function $s_Q(t)$ and a normalized periodic signal $h(s)$ as $g(t) = h(s_Q(t))$. In addition, given another phase evolution function $s'_Q(t) (\neq s_Q(t))$, we can consider another normalized periodic signal $h'(s)$ which satisfied $h'(s) = g(s'_Q^{-1}(s))$. This means that the quasi-periodic signal $g(t)$ is also derived from a combination of a phase evolution function $s'_Q(t)$ and a normalized periodic signal $h'(s)$ as $g(t) = h'(s'_Q(t))$. In other word, given the quasi-periodic signal, the combination ambiguity of the phase evolution function and the normalized periodic signal remains as shown in Fig. 3.

This ambiguity is not problematic in cases where the final goal is phase registration or period segmentation; we can adopt one of the combinations of the phase evolution function and normalized periodic signal as the result.

Nevertheless, the ambiguity poses a serious problem in cases where the reconstructed phase evolution function and normalized periodic signal are used for temporal interpolation or temporal super resolution. This is because once the biased phase evolution function and phase-biased normalized periodic signal are reconstructed, the playing speed of the resulting temporally interpolated or super-resolved signal is also biased.

This can also degrade performance of DTW matching between a gallery and a probe signal. Actually, if the normalized

periodic signals of a gallery signal are reconstructed as phase-biased signals due to the biased phase evolution function $s'_Q(t)$, additional effort of elastic phase deformation is needed to match it to a probe signal. This leads to additional transition cost in the DTW matching process, which is essentially unnecessary in the case of a phase-unbiased normalized periodic signal $h(s)$.

Note that the smoothness term in (9) only acts locally, namely, on adjacent samples, and that it does not solve the combination ambiguity.

C. Bias Correction Framework

In this subsection, we provide a bias correction framework to handle the combination ambiguity problem. For this purpose, we make an assumption that a similar tendency of deviations is unlikely to be observed for every period; e.g., phase evolves faster than the linear time evolution in the first half and slower than the linear time evolution in the latter half as shown in $s_Q(t)$ in Fig. 3. We believe this assumption is reasonable due to the occurrence of random fluctuations in many real-world cases (e.g., a network camera with limited communication bandwidth) or fluctuations in the periodic signal itself (e.g., fluctuations in human walking patterns of healthy people). As an implication based on this assumption, we consider that phase fluctuations are unbiased, in other word, phase deviations from a linear phase evolution averaged over all the periods (i.e., bias) should be zero. As a conclusion, we therefore incorporate the assumption into the optimization framework. Because phase bias computation and phase estimation requires each other's result, we introduce an iterative optimization framework as described below.

After we obtain an initial estimate of the phase sequence, we compute a time warping function (TWF) which represents a mapping from a linear time evolution to the estimated relative phase for each period. Once the bias of the TWFs are computed from phase sequence estimate S_Q^r at the r -th iteration, an unbiased phase $\hat{s}_{Q,i}^r$ at the r -th iteration is then computed based on the TWFs for each sample. This bias-correction term is subsequently defined as a sum of squared differences between the phase estimate $s_{Q,i}^{r+1}$ at the $(r+1)$ -th iteration and the unbiased phase $\hat{s}_{Q,i}^r$ at the r -th iteration for each sample, which is incorporated in the global optimization framework. More details of individual steps are described below.

D. Formulation

In this section, the global and iterative optimization framework is reformulated, where superscript r denotes r -th iteration. As described before, the phase evolution sequence S_Q^{r+1} at the $(r+1)$ -th iteration is estimated by taking into consideration not only three points mentioned in Section IV but also the bias-correction term $D_b(S_Q^{r+1}; \hat{S}_Q^r)$ as

$$S_Q^{r+1*} = \arg \min_{S_Q^{r+1}} D' \left(S_Q^{r+1}; \hat{S}_Q^r \right) \quad (31)$$

$$D' \left(S_Q^{r+1}; \hat{S}_Q^r \right) = D_d \left(S_Q^{r+1} \right) + \lambda_s D_s \left(S_Q^{r+1} \right) + \lambda_b D_b \left(S_Q^{r+1}; \hat{S}_Q^r \right) \quad (32)$$

$$D_b \left(S_Q^{r+1}; \hat{S}_Q^r \right) = \sum_{i=0}^N \left(s_{Q,i}^{r+1} - \hat{s}_{Q,i}^r \right)^2 \quad (33)$$

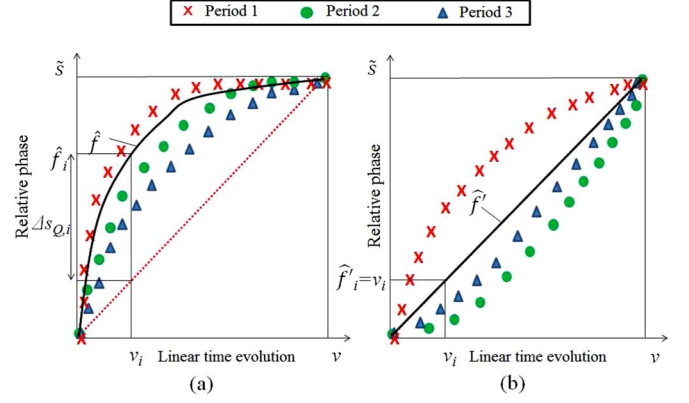


Fig. 4. TWF and bias correction. (a) TWF before bias correction, (b) TWF after bias correction.

$$\text{subject to } s_{Q,i+1}^{r+1} - s_{Q,i}^{r+1} \geq 0 \quad \forall i = 0, \dots, N-2, \quad (34)$$

where λ_b is a coefficient for the bias-correction term.

Finally, because the reformulated objective function $D'(S_Q^{r+1}; \hat{S}_Q^r)$ is a quadratic form and the constraints of (34) and (15) are linear forms with respect to S_Q^{r+1} , the above optimization problem is efficiently solved by convex quadratic programming using the active set method.

E. TWF

Once the phase sequence has been estimated, we can obtain period segmentation boundaries in sub-sampling order given that phase s and relative phase \tilde{s} are, respectively, integers and zero values at the period segmentation boundaries. In more detail, the j -th period segmentation boundary $i_{\text{bound}}^{(j)}$ is obtained as follows. First, we find a pair of adjacent samples $[i^{(j)}, i^{(j)} + 1]$ around the period boundary that satisfies

$$(s_{Q,i^{(j)}} - j)(s_{Q,i^{(j)}+1} - j) \leq 0. \quad (35)$$

Next, the j -th period segmentation boundary $i_{\text{bound}}^{(j)}$ is calculated by interpolation as

$$i_{\text{bound}}^{(j)} = (1 - w^{(j)})i^{(j)} + w^{(j)}(i^{(j)} + 1) \quad (36)$$

$$w^{(j)} = \frac{j - s_{Q,i^{(j)}}}{s_{Q,i^{(j)}+1} - s_{Q,i^{(j)}}}. \quad (37)$$

Furthermore, the linear time evolution v_i for the i -th sample within a period, is defined as

$$v_i = \frac{i - i_{\text{bound}}^{(\lfloor s_{Q,i} \rfloor - 1)}}{i_{\text{bound}}^{(\lfloor s_{Q,i} \rfloor)} - i_{\text{bound}}^{(\lfloor s_{Q,i} \rfloor - 1)}}. \quad (38)$$

As described previously, the TWF expresses the mapping from the linear time evolution v to an estimated relative phase \tilde{s}_Q , as illustrated in Fig. 4, with that for the j -th period denoted as $\tilde{s} = w^{(j)}(v)$. Note that the continuous mapping function $w^{(j)}(v)$ is not directly acquired. Instead, sampled pairs of the linear time evolution parameter and the relative phase within the j -th period are given as $W^{(j)} = \{[v_i, \tilde{s}_{Q,i}] | \lfloor s_{Q,i} \rfloor = j\}$.

F. Bias Estimation

One of simple ideas to estimate the bias from the linear time evolution is to compute a subtraction between an average of multiple-period TWF $\{w^{(j)}(v)\}$ and the linear time evolution. This is, however, difficult because the continuous TWFs $w^{(j)}(v)$ cannot be used and different samples of the linear time evolution v_i are observed among the periods. Moreover, it is not guaranteed that sampled pairs of the linear time evolution and the relative phase $\{[v_i, \tilde{s}_{Q,i}]\}$ lies on a single TWF due to deviations for individual periods, as shown in Fig. 4(a).

Therefore, a cubic-order natural spline function $f(v; \theta)$ on the linear-time evolution v is introduced to represent a continuous TWF, with θ denoting the parameters for the spline function. These are estimated so as to minimize the following objective function composed of the data fitness term to the sampled pairs $\{[v_i, \tilde{s}_{Q,i}]\}$ and tension and stiffness terms of the spline curve as

$$D(\theta) = \frac{1}{N} \sum_{i=0}^{N-1} (f(v_i; \theta) - \tilde{s}_{Q,i})^2 + \lambda_{\text{tense}} \int_0^1 \left\| \frac{df}{dv} \right\|^2 dv + \lambda_{\text{stiff}} \int_0^1 \left\| \frac{d^2f}{dv^2} \right\|^2 dv, \quad (39)$$

where λ_{tense} and λ_{stiff} are coefficients for the tension and stiffness, respectively. Once the spline parameters are estimated, a biased relative phase for i -th sample is interpolated by the spline function as \hat{f}_i and a bias correction amount $\Delta s_{Q,i}$ is then computed as

$$\Delta s_{Q,i} = \hat{f}_i - v_i. \quad (40)$$

Finally, the unbiased absolute phase is computed as

$$\hat{s}_{Q,i} = s_{Q,i} - \Delta s_{Q,i}. \quad (41)$$

G. Algorithm Summary

The global optimization is finally processed iteratively as described in the following.

- **Step 1**
Set the iteration index r to 0 and compute an initial solution of phase sequence S_Q^0 by the convex quadratic programming composed of the objective function $D(S_Q^0)$ (9) and the constraints ((12) and (15)).
- **Step 2**
Estimate the spline function of the TWF by minimizing (39) based on the phase sequence S_Q^r and compute the unbiased phase \hat{S}_Q^r using (40) and (41).
- **Step 3**
Update the phase sequence S_Q^{r+1} by the convex quadratic programming composed of the objective function $D'(S_Q^{r+1}; \hat{S}_Q^r)$ ((31)) and the constraints ((34) and (15)) based on the unbiased phase \hat{S}_Q^r .
- **Step 4**
Increment iteration index r and then go back to Step 1 if $r \leq r_{\text{max}}$, otherwise, terminate the iteration.

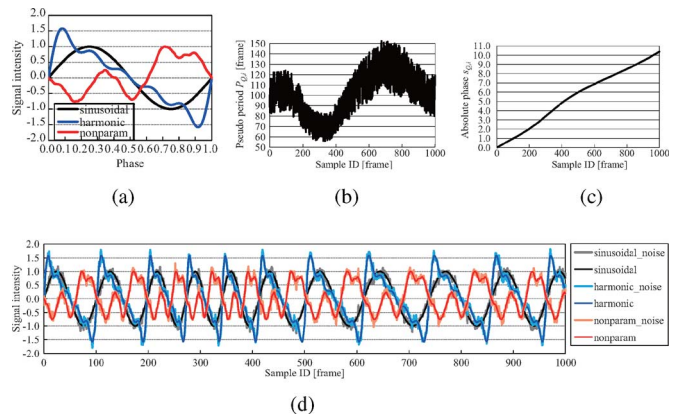


Fig. 5. Signals in the simulation data. (a) Normalized periodic signals. (b) Instantaneous period. (c) Phase evolution sequence. (d) Quasi-periodic signals.

VI. EXPERIMENTS USING SIMULATION DATA

A. Dataset

To confirm the effectiveness of the proposed phase estimation, we conducted experiments using simulation data⁴.

First, we generated three normalized periodic signals with a common parameter, s , from the sinusoidal function $h(s) = \sin(2\pi s)$, the harmonic-sum function $h(s) = \sum_{k=1}^5 (1/k) \sin(2\pi ks)$ with k set to 5, and a non-parametric function constructed from the second-order differential (d^2h/ds^2) of an $h(s)$ randomly drawn from a uniform distribution in the domain $[-500, 500]$ and with periodic boundary conditions $h(1) = h(0) = 0$. The generated normalized periodic signals are shown in Fig. 5(a).

Second, the phase evolution function $s_Q(t)$ was also generated by a non-parametric scheme in the same way. A instantaneous period $P_Q(t)$ was generated with a second-order differential (d^2P_Q/dt^2) drawn from a uniform distribution in the domain $[-0.25, 0.25]$, boundary conditions $P_Q(0) = P_Q(T) = P$, where T is the time at the final frame and P is a predefined period, and additive noise drawn from a uniform distribution in the domain $[-0.2P, 0.2P]$. The phase evolution function $s_Q(t)$ is then given by the first-order differential equation $ds_Q/dt = 1/P_Q(t)$ with initial condition $s_Q(t) = 0$. In the simulation, T and P were set to 10 and 100, respectively. The generated instantaneous period $P_Q(t)$ and phase evolution sequence $s_Q(t)$ are shown in Figs. 5(b) and (c), respectively. As shown by Fig. 5(b), local phase fluctuations as well as global phase modulations are included in the generated phase evolution sequence.

Third, quasi-periodic signals were generated by sampling at $(1/P)$ intervals as $g_i = h(s_Q(it/P))$, $i = 0, \dots, N$, where $N = TP$ is the sample ID in the final frames. Fourth, sequences with signal intensity noise were also generated as $g'_i = g_i + \delta$, where δ is drawn from a Gaussian distribution with standard deviation $\sigma = 0.1$. The generated quasi-periodic signals are shown in Fig. 5(d). The other parameters used in each process were set experimentally as $\alpha = 1.0$, $\beta = 0.3$, $\lambda_s = 10.0$, and $\lambda_b = 1000.0$. We set the maximum iteration r_{max} to 2.

⁴Software and dataset can be accessed here: <http://www.am.sanken.osaka-u.ac.jp/research/SelfDTW.html>

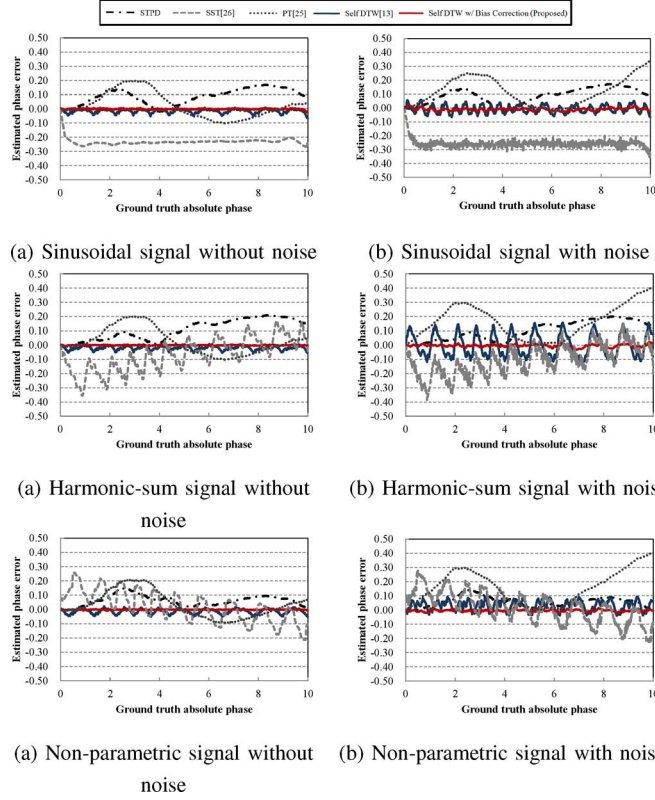


Fig. 6. Estimated phase error on simulated signals.

B. Benchmark Methods

Because a reference signal is not given, as stated in Section III, most of the existing methods such as continuous cyclic DP and cyclic HMM cannot be applied. Therefore, we regard the following scheme, based on the estimated instantaneous period with STPD, as a baseline algorithm for comparison:

$$s_{Q,i+1} = s_{Q,i} + \frac{1}{\hat{P}_{Q,i}}, \quad (42)$$

where we initialize $s_{Q,0} = 0$. Note that, in the proposed framework, this is also equivalent to setting the regularization coefficient λ_s to infinity.

We also implemented the SST [25], [47]⁵ and period trace (PT) [28], and estimate the phase by recurrence formula ((42)) in the same way as STPD.

C. Phase Estimation Results

First, we evaluated the errors between the estimated phase and the ground truth in Fig. 6. Note that phase errors should be evaluated by variance or standard deviation without a mean component of the errors because constant phase shift \bar{s} is meaningless, as discussed in Section IV.

As for only Self DTW [13], although the phase error variance is large to a certain extent, the phase error patterns are still similar to a quasi-periodic form; this implies the possibility that a combination of a biased phase evolution $s_Q(t)$ and a phase-biased normalized periodic signal $h(s)$ has been reconstructed. For example, given a harmonic-sum signal without noise, a reconstructed spline function of TWF is biased from

⁵We used SST toolbox provided in [48].

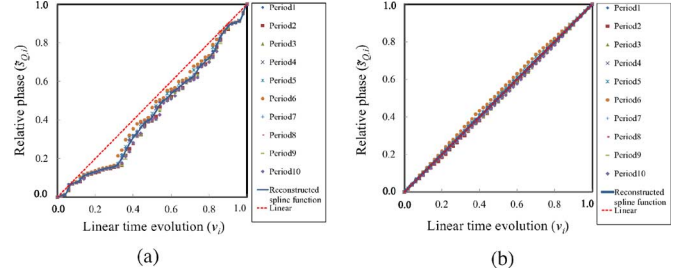


Fig. 7. TWF for harmonic-sum signal without noise before and after bias correction. (a) Before bias correction. (b) After bias correction.

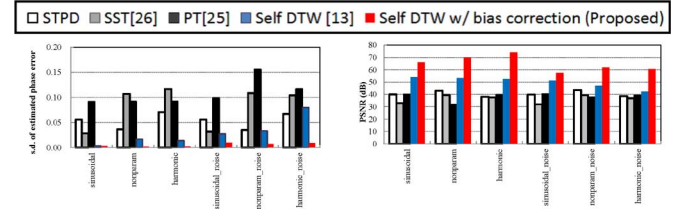


Fig. 8. Standard deviation of estimated phase error (left) and PSNR of phase registration results (right).

linear phase evolution, as shown in Fig. 7(a). Thus, these quasi-periodic phase errors can effectively be removed by bias correction, as shown in Figs. 6 (self DTW w/ bias correction) and 7(b). In addition, this trend is common for signals with intensity noise although the phase error variances are naturally larger than those for signals without intensity noise (Fig. 6(b)).

In contrast, the error variance in the other benchmark methods (STPD, SST, PT) is larger than that in the proposed methods due to accumulation errors, and furthermore, the error patterns do not resemble a quasi-periodic form.

To summarize the phase estimation performance, the standard deviations are shown in Fig. 8(left). As a result, we can see that the estimated phase errors are sufficiently reduced when using self DTW together with bias correction.

D. Phase Registration Results

Next, phase registration results for the harmonic-sum signal without intensity noise were evaluated by plots of the relative phase $\tilde{s}_{Q,i}$ and the corresponding signal intensity g_i in Fig. 9. Note that these plots form a certain normalized periodic signal $h(s)$ if the phase is correctly registered.

According to the result, the plots for self DTW [13] lie on a single curve and form a similar curve to the ground truth signal except for phase bias. This shows that self DTW even without bias correction is sufficient for the purpose of phase registration or period segmentation in sub-sampling order. Moreover, the plots for self DTW with bias correction lie almost on the ground truth signal without any phase bias, and hence self DTW with bias correction enables further applications such as time interpolation and temporal super resolution from a single quasi-periodic signal. In contrast, the plots of the other benchmark methods are widely distributed around the ground truth signals due to incorrect phase estimation.

To summarize the phase registration performance, the peak-signal-to-noise ratio (PSNR) is shown in Fig. 8(right). As we can see, the self DTW with bias correction gives better phase

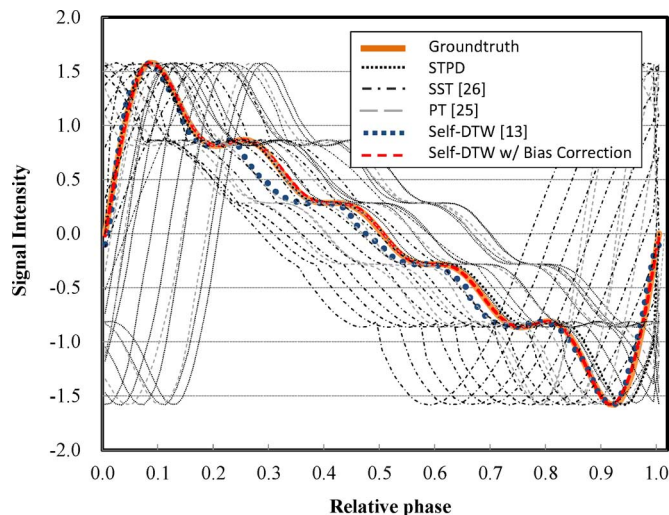


Fig. 9. Phase registration results for harmonic-sum signal.

registration results than STPD, SST [25], PT [28], and self DTW only [13].

E. Effect of Smoothness and Bias Correction Term Coefficients

In this subsection, the effect of smoothness and the bias correction coefficient, λ_s and λ_b , on estimated phase errors is investigated for the harmonic-sum signal.

On the one hand, adopting small λ_s values (e.g., 1 or 10), the phase evolution curve tends to be flexible. Thus, while it can effectively absorb local phase fluctuations, it suffers from phase bias due to the combination ambiguity problem of the phase sequence and normalized periodic signal, and the magnitude of the estimated phase errors increases as λ_s decreases, as shown in Fig. 10. These error patterns are, however, almost of quasi-periodic form as seen in Fig. 10(a), and hence they are effectively removed by adding the bias-correction term as shown in Figs. 10(b),(c),(d), and 11.

On the other hand, adopting large λ_s values (e.g., 1000 or 10000), the phase evolution curve tends to be stiff. Thus, while it is robust to such quasi-periodic phase errors even if only self DTW is used, it cannot correctly absorb local phase fluctuations and/or middle-range phase modulations particularly given a fairly large λ_s (e.g., 10000), which results in relatively large phase estimation errors compared with the middle λ_s (e.g., 100), as shown in Fig. 11.

In summary, as long as self DTW is used together with a small or middle-range smoothness coefficient λ_s (e.g., from 1 to 100 in this example) and a sufficiently large bias correction coefficient λ_b (from 100 to 10000), the estimated phase errors are suppressed within a certain satisfactory range with more stability and smoothness.

VII. APPLICATIONS TO REAL VISION DATA

A. Phase Alignment for Viewpoint-Transited Gait Silhouettes Sequence

We conducted an experiment on two types of gait silhouette sequences under viewpoint transition; one is selected from a gallery set of the USF Gait Database (call it USF later) [6] and

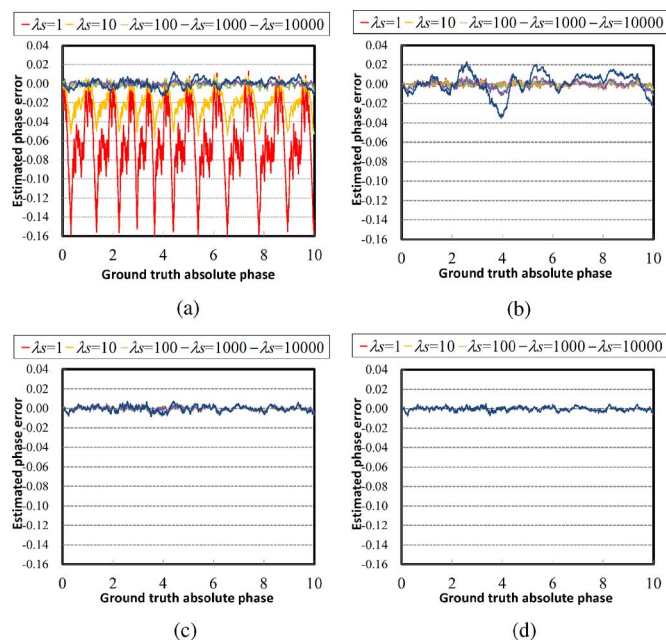


Fig. 10. Effect of regularization term coefficients λ_s and λ_b on estimated phase error for harmonic-sum signal. (a) Self DTW [13]. (b) Self DTW w/ bias correction ($\lambda_b = 1$). (c) Self DTW w/ bias correction ($\lambda_b = 100$). (d) Self DTW w/ bias correction ($\lambda_b = 10000$).

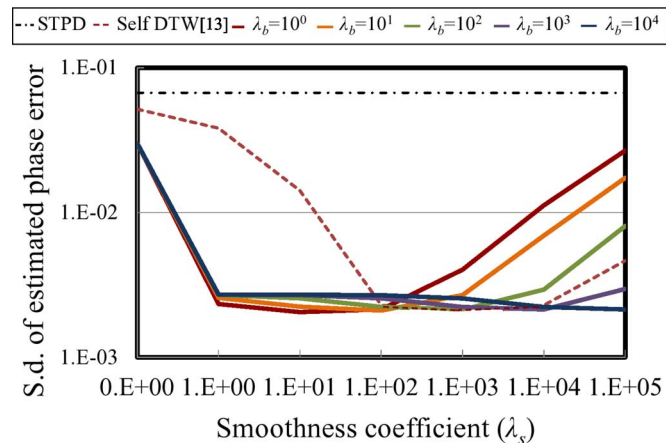


Fig. 11. Effect of smoothness coefficient λ_s and bias correction coefficient λ_b on standard deviation of estimated phase error for harmonic-sum signal.

the other from the OU-ISIR Gait Database, the large population dataset (call it OULP later) [49]. While USF contains slight viewpoint change within a sequence and its silhouette quality is relatively poor due to outdoor environment, OULP contains relatively large view point change (front-oblique to side view) but with relatively fine silhouette quality. Size-normalized (88 by 128 pixels) gait silhouette sequences at 30 fps were provided for both USF and OULP. Each gait silhouette was converted into an unfolded image vector whose dimension is image size in a raster scan way, and it was further projected into a lower dimensional vector g by principal component analysis (PCA). A sequence of such lower dimensional vectors $G = \{g_i\}$ was used as an input quasi-periodic signal.

Figs. 12 and 13 show the gait silhouette images aligned at the estimated relative phase. Despite the low silhouette quality in USF and viewpoint changes in OULP, all gait phases, such

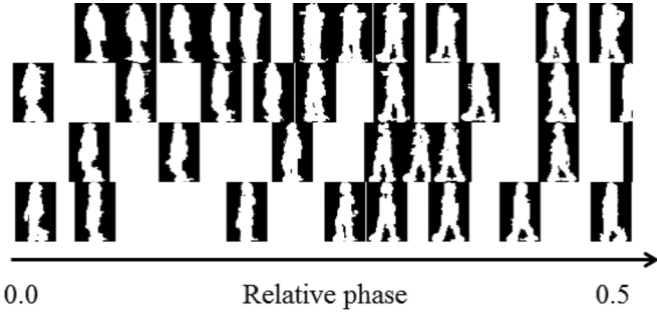


Fig. 12. Multiple gait silhouette images from USF aligned at the estimated phases (every 2 frames, a half gait period). The horizontal axis indicates the relative phase \bar{s} and each silhouette image is aligned at the estimated relative phase.

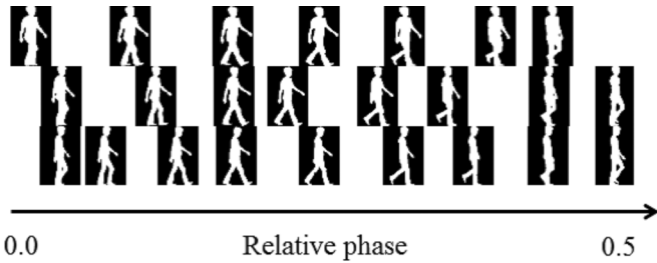


Fig. 13. Multiple gait silhouette images from OULP aligned at the estimated phases (every 2 frames, a half gait period). The horizontal axis indicates the relative phase \bar{s} and each silhouette image is aligned at the estimated relative phase.

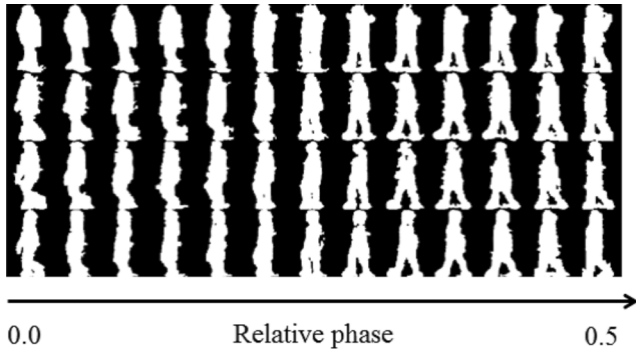


Fig. 14. A half gait period of a phase normalized gait silhouette sequence from USF. The horizontal axis indicates the relative phase \bar{s} and each silhouette image is aligned at the relative normalized phase (every 4 frames).

as the double-support phase and single-support phase, are well registered among periods.

With a view to applications, phase-registered image sequences are quite useful. For example, a phase-normalized gait silhouette sequence can be produced from the temporal interpolation of the estimated phase information so that the intervals between adjacent silhouette images are uniform, as illustrated in Figs. 14 and 15. Such sequences can be useful in reducing the effects of frame misalignment due to temporal rate difference during the matching process in gait recognition.

B. Manifold Reconstruction From Speed-Transited Gait Silhouette Sequence

We also conducted an experiment on a gait silhouette sequence with gradual speed variations ranging from 6 km/h to

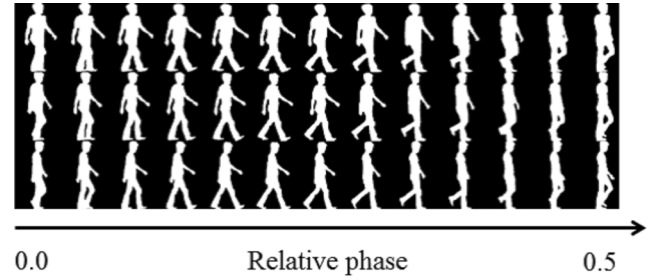


Fig. 15. A half gait period of a view-transited phase normalized gait silhouette sequence from OULP. The horizontal axis indicates the relative phase \bar{s} and each silhouette image is aligned at the relative normalized phase (every 4 frames).

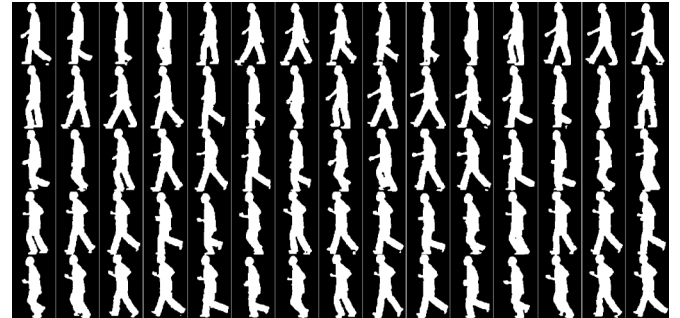


Fig. 16. Sub-sequences of input gait silhouettes from OUTD (every 4 frames). Top to bottom rows correspond to 6, 7, 8, 9, and 10 km/h, respectively. Note that the phases between different walking speeds are not synchronized.

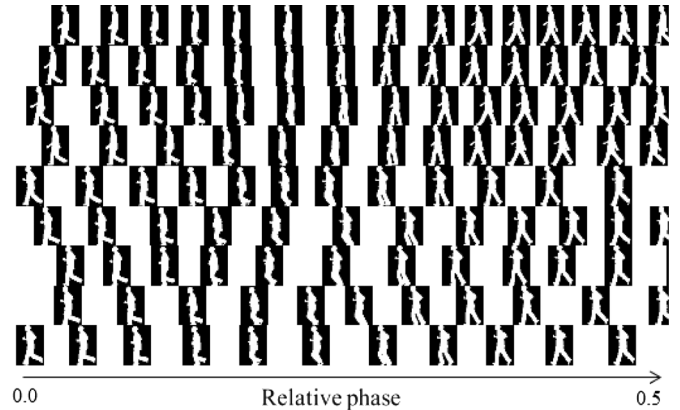


Fig. 17. Multiple gait silhouette images from OUTD aligned at the estimated phases (every 2 frames, a half gait period). The horizontal axis indicates the relative phase \bar{s} and each silhouette image is aligned at the estimated relative phase. The vertical axis indicates the number of periods (every 5 periods). Changes in the rows from top to bottom represent a gradual speed increase from 6 km/h to 10 km/h.

10 km/h (Fig. 16), selected from the publicly available OU-ISIR Gait Database, the treadmill dataset A (call it OUTD later) [50]. A size-normalized silhouette sequence (88 by 128 pixels) at 60 fps are provided. In the same way as the previous subsection, a sequence of such lower dimensional vectors $G = \{g_i\}$ in the PCA space was used as an input quasi-periodic signal.

Fig. 17 shows the gait silhouette images aligned at the estimated relative phase and Fig. 18 shows a phase-normalized gait silhouette sequence. Despite the significant variation in gait

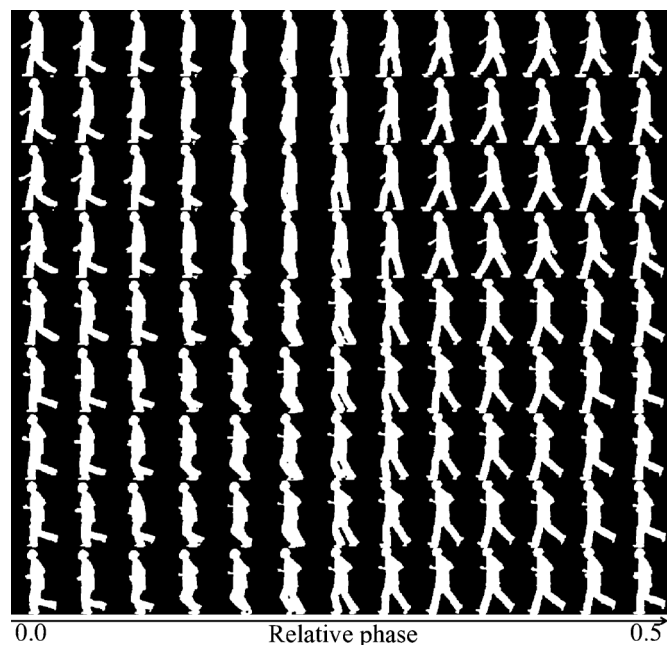


Fig. 18. A half gait period of a phase normalized gait silhouette sequence from OUTD. The horizontal axis indicates the relative phase \bar{s} and each silhouette image is aligned at the relative normalized phase (every 4 frames). The vertical axis indicates the number of periods (every 5 periods). Changes in the rows from top to bottom represent a gradual speed increase from 6 km/h to 10 km/h.

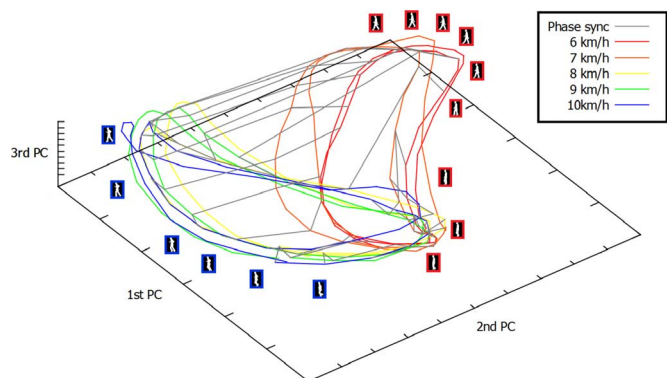


Fig. 19. A 2D gait manifold parameterized by phase and walking speed. Each colored loop depicts a manifold for a single walking speed parameterized by phase, while gray lines represent phase synchronization among the walking speeds.

style due to large speed variations from walking (6 km/h) to running (10 km/h), all gait phases are well registered for the different speeds.

Furthermore, given just a single walking sequence with speed variation, a gait manifold parameterized by both phase and walking speed can be constructed by the phase-normalized speed-varied gait image sequence (see Fig. 19). The gait manifold enables us to analyze the gait pose transition by walking speed for fixed phase as well as by phase for fixed walking speed.

Moreover, in the context of gait recognition with speed variations, the 2D gait manifold is provided as an efficient gallery expression, unlike the existing 1D gait manifold parameterized only by phase [31]. A set of 1D gait manifolds with different speeds, depicted as colored loops in Fig. 19, cannot deal with

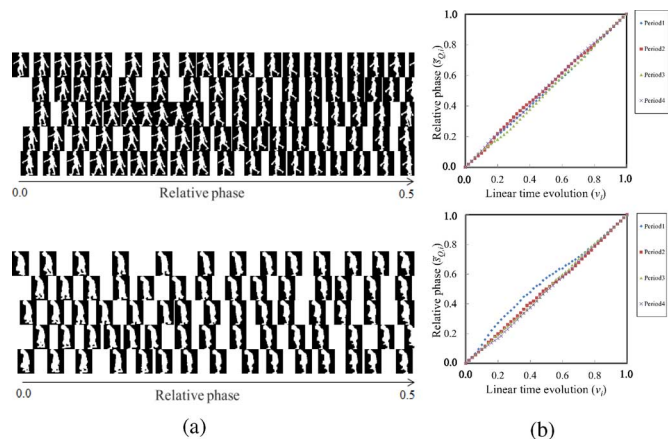


Fig. 20. Variance in TWFs as the phase evolution instability measure. Time warping function variance between periods for unstable gait (bottom) is larger than that for stable gait (top). (a) Half gait-period of multiple silhouette images aligned by estimated relative phase. (b) TWFs.

variations in walking speed within a period, as these do not provide phase registration information across different walking speeds, depicted as gray lines in Fig. 19. In contrast, because a 2D gait manifold has such phase registration information across different walking speeds, it can appropriately match a sequence with walking speed variations within a period in the framework of 1D-2D (input to gallery) dynamic programming. Note that the proposed method is applicable not only to gait with speed variation, but also to general quasi-periodic signals undergoing transition by factors other than phase, such as periodic action recognition with gradual view changes or periodic signal analysis with gradual attenuation⁶.

C. Phase Evolution Instability Measure

Because the proposed method reconstructs TWFs from a single quasi-periodic signal through a bias estimation process, the variance in the reconstructed TWFs can be used as a kind of phase evolution instability measure of the signal. For example, gait silhouettes of two subjects aligned by estimated relative phase are shown together with their reconstructed TWFs in Fig. 20. Note that the non-uniform alignment intervals of these gait silhouette images represent a non-linear time distortion due to the gait fluctuation obtained by the proposed method. We can see that the phase intervals for the first subject (top of Fig. 20) are almost constant across periods and we can say that this subject's phase evolution is stable. As such, the variance in reconstructed TWFs for the first subject is small. In contrast, the phase intervals for the second subject (bottom of Fig. 20) differ greatly across periods at several relative phases and thus the phase evolution is unstable. As a result, the variance in reconstructed TWFs for the second subject is larger than that for the first subject.

Therefore, the variances in TWFs can be exploited as a kind of phase evolution instability measure, which could be a potential feature in gait-based person identification or age group classification for example, because a child's gait is more unstable than that of an adult. Note that previous DTW-based

⁶In these cases, the manifold is parameterized by phase and view or degree of attenuation.

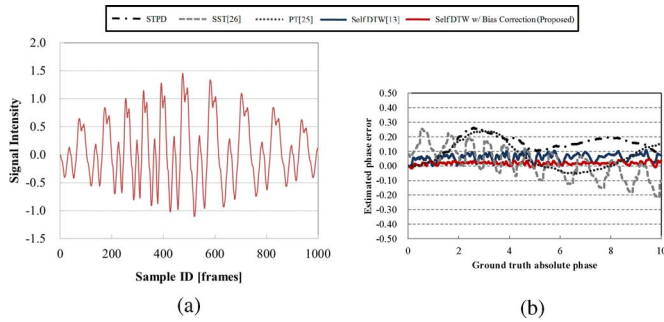


Fig. 21. Input and result with non-parametric signal with AM and FM. (a) Input signal. (b) Phase estimation errors.

TABLE I

COMPARISON ON STANDARD DEVIATION OF PHASE ESTIMATED ERROR ON NON-PARAMETRIC SIGNAL WITH AND WITHOUT AM

Signal	STPD	SST[25]	PT[28]	Self DTW[13]	Proposed
Without AM	0.036	0.107	0.092	0.017	0.001
With AM	0.064	0.108	0.093	0.025	0.018

methods need the reference signal period in addition to an input quasi-periodic signal to obtain these TWFS, whereas the proposed method needs only a single input quasi-periodic signal.

VIII. DISCUSSION AND LIMITATIONS

Signal With AM and FM: In order to see the effect of AM in quasi-periodic signal on the proposed method, we also carried out the experiment non-parametric simulated signal with AM as well as FM (Fig. 21(a)). From Fig. 21(b) and Table I, while the phase estimation error for the signal with AM and FM increases compared with that for the signal only with FM. Nevertheless, the increase of the phase estimation error of the proposed method is limited compared with those of the other methods. This shows the potential robustness of the proposed method against AM as well as FM and signal noise.

Low Sampling Rate: The accuracy of the correspondences between a quasi-periodic signal and a multiple-period shifted signal used in the proposed self DTW process is highly dependent on the sample density within a period. This is because both relative phases and similar signal intensities between the corresponding pair are quite similar in the case where signals are densely sampled for each period; in other words, the correspondence is sufficiently accurate. However, no accurate correspondences are obtained when signals are sparsely sampled for each period (e.g., a few samples per period); in this case, the obtained correspondences are inaccurate. Therefore, the proposed method cannot guarantee high phase-estimation performance for signals with low sampling rates.

Rapid Change in Other Factors: If a factor other than phase (e.g., walking speed in a gait silhouette sequence) changes rapidly between adjacent periods, the correspondence pair for self DTW cannot be accurately determined because signal intensity could also change between periods. Therefore, the other factors need to change gradually across periods, as shown in the examples in Section VII.

IX. CONCLUSION

In this paper, we proposed a method for phase estimation of a single non-parametric quasi-periodic signal. Having detected a short-term period for each sample by normalized autocorrelation, correspondences of multiple-period shifts are obtained by self DTW and these are used in the subsequent phase optimization framework. Reconstructed phase evolution functions are often biased due to the combination ambiguity of the phase evolution function and normalized periodic signal, and thus the bias-correction term is incorporated into the proposed algorithm to correct such phase bias.

Future work includes extensions of the proposed method to quasi-periodic signals with multiple AM and FM components, and applications to matching and time super-resolution of quasi-periodic signals.

REFERENCES

- [1] D. Newkirk and R. Karlquist, *Communication Systems*, 2nd ed. New York, NY, USA: McGraw-Hill, 1981.
- [2] J. B. Anderson, T. Aulin, and C.-E. Sundberg, *Digital Phase Modulation*. New York, NY, USA: Springer, 1986.
- [3] F. Liu and R. Picard, "Finding periodicity in space and time," in *Proc. 6th Int. Conf. Comput. Vis.*, 1998, pp. 376–383.
- [4] A. Briassouli and N. Ahuja, "Estimation of multiple periodic motions from video," in *Proc. 9th Eur. Conf. Comput. Vis.*, 2006, pp. 147–159.
- [5] X. Feng and P. Perona, "Human action recognition by sequence of movelet codewords," in *Proc. 1st Int. Symp. 3D Data Process. Visual. Transmission*, Los Alamitos, CA, USA, 2002, pp. 717–721.
- [6] S. Sarkar, J. Phillips, Z. Liu, I. Vega, P. Grother, and K. Bowyer, "The humanid gait challenge problem: Data sets, performance, and analysis," *IEEE Trans. Pattern Anal. Mach. Intell.*, vol. 27, no. 2, pp. 162–177, 2005.
- [7] A. M. Y. Makihara and Y. Yagi, "Periodic temporal super resolution based on phase registration and manifold reconstruction," *IPSJ Trans. Comput. Vis. Appl.*, vol. 3, pp. 134–147, Dec. 2011.
- [8] J. van Ouwerkerk, "Image super-resolution survey," *Image Vis. Comput.*, vol. 24, no. 10, pp. 1039–1052, Oct. 2006.
- [9] C. S. Lee and A. Elgammal, "Simultaneous inference of view and body pose using torus manifolds," in *Proc. 18th Int. Conf. Pattern Recognit.*, Hong Kong, China, Aug. 2006, vol. 3, pp. 489–494.
- [10] N. Trung, Y. Makihara, H. Nagahara, R. Sagawa, Y. Mukaigawa, and Y. Yagi, "Phase registration in a gallery improving gait authentication," in *Proc. Int. Joint Conf. Biometrics (IJCB)*, Washington, DC, USA, Oct. 2011, pp. 1–7.
- [11] H. Sakoe and S. Chiba, "Dynamic programming algorithm optimization for spoken word recognition," *IEEE Trans. Acoust., Speech, Signal Process.*, vol. 26, no. 1, pp. 43–49, 1978.
- [12] R. Oka, "Spotting method for classification of real world data," *Comput. J.*, vol. 41, no. 8, pp. 559–565, 1998.
- [13] Y. Makihara, N. Trung, H. Nagahara, R. Sagawa, Y. Mukaigawa, and Y. Yagi, "Phase registration of a single quasi-periodic signal using self dynamic time warping," in *Proc. 10th Asian Conf. Comput. Vis.*, Queenstown, New Zealand, Nov. 2010, pp. 1965–1975.
- [14] D. Aronsson, E. Bjornemo, and M. Johansson, "Estimation and detection of a periodic signal," in *Proc. Amer. Inst. Phys. Conf., Bayesian Inference Maximum Entropy Methods in Sci. Eng.*, 2006, vol. 872, pp. 139–146.
- [15] V. Znak, "Some aspects of estimating the detection rate of a periodic signal in noisy data and the time position of its components," *Pattern Recognit. Image Anal.*, vol. 19, no. 3, pp. 539–545, Sep. 2009.
- [16] P. Handel and P. Tichavsky, "Adaptive estimation for periodic signal enhancement and tracking," *Int. J. Adapt. Control Signal Process.*, vol. 8, no. 5, pp. 447–456, Mar. 2007.
- [17] M. Betser, P. Collen, G. Richard, and B. David, "Estimation of frequency for am/fm models using the phase vocoder framework," *IEEE Trans. Signal Process.*, vol. 56, no. 2, pp. 505–517, Feb. 2008.
- [18] A. K. Barros and N. Ohnishi, "Amplitude estimation of quasiperiodic physiological signals by wavelets," *IEICE Trans. Inf. Syst.*, vol. E83-D, no. 12, pp. 2193–2195, Dec. 2000.
- [19] M. Morelande, "Parameter estimation of phase-modulated signals using Bayesian unwrapping," *IEEE Trans. Signal Process.*, vol. 57, no. 11, pp. 4209–4219, Nov. 2009.

- [20] P. O'Shea, "Improving polynomial phase parameter estimation by using nonuniformly spaced signal sample methods," *IEEE Trans. Signal Process.*, vol. 60, no. 7, pp. 3405–3414, Jul. 2012.
- [21] S. Aviyente and A. Mutlu, "A time-frequency-based approach to phase and phase synchrony estimation," *IEEE Trans. Signal Process.*, vol. 59, no. 7, pp. 3086–3098, Jul. 2011.
- [22] P. Gruber and J. Todtli, "Estimation of quasiperiodic signal parameters by means of dynamic signal models," *IEEE Trans. Signal Process.*, vol. 42, no. 3, pp. 552–562, Mar. 1994.
- [23] M. Nakashizuka, "A sparse decomposition method for periodic signal mixtures," *IEICE Trans. Fundam. Electron., Commun., Comput. Sci.*, vol. E91-A, no. 3, pp. 791–800, Mar. 2008.
- [24] H. Wong and W. A. Sethares, "Estimation of pseudo-periodic signals," in *Proc. IEEE Int. Conf. Acoust., Speech, Signal Process.*, May 2004, vol. 2, pp. 557–560.
- [25] "Synchrosqueezed wavelet transforms: An empirical mode decomposition-like tool," *Appl. Comput. Harmon. Anal.*, vol. 30, no. 2, pp. 243–261, 2011.
- [26] Y.-C. Chen, M.-Y. Cheng, and H.-T. Wu, "Nonparametric and adaptive modeling of dynamic seasonality and trend with heteroscedastic and dependent errors," *ArXiv e-prints*, Oct. 2012 [Online]. Available: <http://arxiv.org/abs/1210.4672>
- [27] H. Tieng Wu, "Instantaneous frequency and wave shape functions (i)," *Appl. Comput. Harmon. Anal.*, vol. 35, no. 2, pp. 181–199, 2012.
- [28] S. S. Seitz and C. R. Dyer, "Detecting irregularities in cyclic motion," in *Proc. Workshop Motion Non-Rigid Articulated Objects*, 1994, pp. 178–185.
- [29] H. Murase and R. Sakai, "Moving object recognition in eigenspace representation: Gait analysis and lip reading," *Pattern Recognit. Lett.*, vol. 17, pp. 155–162, 1996.
- [30] N. Boulgouris, K. Plataniotis, and D. Hatzinakos, "Gait recognition using linear time normalization," *Pattern Recognit.*, vol. 39, no. 5, pp. 969–979, 2006.
- [31] A. Mori, Y. Makihara, and Y. Yagi, "Gait recognition using period-based phase synchronization for low frame-rate videos," in *Proc. 20th Int. Conf. Pattern Recognit.*, Istanbul, Turkey, Aug. 2010, pp. 2194–2197.
- [32] J. Little and J. Boyd, "Recognizing people by their gait: The shape of motion," *Videre: J. Comput. Vis. Res.*, vol. 1, no. 2, pp. 1–13, 1998.
- [33] Y. Makihara, R. Sagawa, Y. Mukaigawa, T. Echigo, and Y. Yagi, "Gait recognition using a view transformation model in the frequency domain," in *Proc. 9th Eur. Conf. Comput. Vis.*, Graz, Austria, May 2006, pp. 151–163.
- [34] L. Rabiner, A. Rosenberg, and S. Levinson, "Considerations in dynamic time warping algorithms for discrete word recognition," *IEEE Trans. Acoust., Speech, Signal Process.*, vol. 26, no. 6, pp. 575–582, Dec. 1978.
- [35] S. Furui, "A VQ-based preprocessor using cepstral dynamic features for speaker-independent large vocabulary word recognition," *IEEE Trans. Acoust., Speech, Signal Process.*, vol. 36, no. 7, pp. 980–987, Jul. 1988.
- [36] A. Veeraraghavan, R. Chellappa, and A. Roy-Chowdhury, "The function space of an activity," in *Proc. 2006 IEEE Comput. Soc. Conf. Comput. Vis. Pattern Recognit.*, New York, NY, USA, Jun. 2006, vol. 1, pp. 959–966.
- [37] N. Cuntoor, A. Kale, and R. Chellappa, "Combining multiple evidences for gait recognition," in *Proc. IEEE Int. Conf. Acoust., Speech, Signal Process.*, 2003, vol. 3, pp. 33–36.
- [38] S. Levinson, L. Rabiner, and M. Sondhi, "Speaker independent isolated digit recognition using hidden Markov models," in *Proc. IEEE Int. Conf. Acoust., Speech, Signal Process. (ICASSP)*, Apr. 1983, vol. 8, pp. 1049–1052.
- [39] T. Matsui and S. Furui, "Comparison of text-independent speaker recognition methods using VQ-distortion and discrete/continuous HMMS," in *Proc. IEEE Int. Conf. Acoust., Speech, Signal Process. (ICASSP)*, Mar. 1992, vol. 2, pp. 157–160.
- [40] X. Zhou and B. Bhanu, "Integrating face and gait for human recognition," presented at the IEEE Comput. Soc. Workshop Biometrics, New York, NY, USA, Jun. 2006.
- [41] L. Lee, G. Dalley, and K. Tieu, "Learning pedestrian models for silhouette refinement," in *Proc. Int. Conf. Comput. Vis.*, Oct. 2003, vol. 1, pp. 663–670.
- [42] Z. Liu and S. Sarkar, "Effect of silhouette quality on hard problems in gait recognition," *Trans. Syst., Man, Cybern. Part B, Cybern.*, vol. 35, no. 2, pp. 170–183, 2005.
- [43] Z. Liu and S. Sarkar, "Improved gait recognition by gait dynamics normalization," *IEEE Trans. Pattern Anal. Mach. Intell.*, vol. 28, no. 6, pp. 863–876, 2006.
- [44] A. Sunderesan, A. Chowdhury, and R. Chellappa, "A hidden Markov model based framework for recognition of humans from gait sequences," in *Proc. IEEE Int. Conf. Image Process.*, 2003, vol. 2, pp. 93–96.
- [45] R. Li and R. Chellappa, "Spatiotemporal alignment of visual signals on a special manifold," *IEEE Trans. Pattern Anal. Mach. Intell.*, vol. 35, no. 3, pp. 697–715, 2013.
- [46] R. Polana and R. C. Nelson, "Detection and recognition of periodic, nonrigid motion," *Int. J. Comput. Vis.*, vol. 23, pp. 261–282, 1997.
- [47] G. Thakur, E. Brevdo, N. S. FućKar, and H.-T. Wu, "The synchrosqueezing algorithm for time-varying spectral analysis: Robustness properties and new paleoclimate applications," *Signal Process.*, vol. 93, no. 5, pp. 1079–1094, May 2013.
- [48] G. Thakur, E. Brevdo, N. S. FućKar, and H.-T. Wu, "Synchrosqueezing Toolbox (MATLAB) [Online]. Available: <https://web.math.princeton.edu/ebrevdo/synsq/>
- [49] H. Iwama, M. Okumura, Y. Makihara, and Y. Yagi, "The OU-ISIR gait database comprising the large population dataset and performance evaluation of gait recognition," *IEEE Trans. Inf. Forensics Security*, vol. 7, no. 5, pp. 1511–1521, 2012.
- [50] Y. Makihara, H. Mannami, A. Tsuji, M. Hossain, K. Sugiura, A. Mori, and Y. Yagi, "The ou-isir gait database comprising the treadmill dataset," *IPSI Trans. Comput. Vis. Appl.*, vol. 4, pp. 53–62, Apr. 2012.



Yasushi Makihara was born in Japan in 1978, and received the B.S., M.S., and Ph.D. degrees in engineering from Osaka University in 2001, 2002, and 2005, respectively. He is currently an Assistant Professor of the Institute of Scientific and Industrial Research, Osaka University. His research interests are gait recognition, morphing, and temporal super resolution. He is a member of IPSJ, RJS, and JSME.



Muhammad Rasyid Aqmar received his B.E. in engineering physics from Institut Teknologi Bandung in 2006. He received his M.E. and Ph.D. degrees in computer science from Tokyo Institute of Technology, in 2009 and 2013, respectively. He is currently a postdoctoral researcher the Department of Intelligent Media, Institute of Scientific and Industrial Research, Osaka University. His research interests include gait recognition and video-based pattern recognition.



Ngo Thanh Trung received his M.E. and Ph.D. degrees from Osaka University in 2005 and 2010, respectively. He is currently working as a postdoctoral researcher in the Department of Intelligent Media, Institute of Scientific and Industrial Research, Osaka University. His research interests include pattern recognition, gait motion recognition, robot localization and 3D map building, omnidirectional vision, and statistical robust estimation methods.



Hajime Nagahara (M'12) received the B.E. and M.E. degrees in electrical and electronic engineering from Yamaguchi University in 1996 and 1998, respectively, and the Ph.D. degree in system engineering from Osaka University in 2001. He was a research associate of the Japan Society for the Promotion of Science (2001–2003). He was an assistant professor at the Graduate School of Engineering Science, Osaka University, Japan (2003–2010). He was a visiting associate professor at CREA University of Picardie Jules Verns, France,

in 2005. He was a visiting researcher at Columbia University in 2007–2008. Since 2010, he has been an associate professor in faculty of information science and electrical engineering at Kyushu University. Computational photography, computer vision, and virtual reality are his research areas. He received an ACM VRST2003 Honorable Mention Award in 2003 and IPSJ Nagao Special Researcher Award in 2012.



Ryusuke Sagawa (M'04) is a senior researcher at Service Robotics Research Group, Intelligent Systems Research Institute, National Institute of Advanced Industrial Science and Technology (AIST), Japan. He received a B.E. in information science from Kyoto University in 1998. He received a M.E. in information engineering in 2000 and Ph.D. in information and communication engineering from the University of Tokyo in 2003. He was an assistant professor at the Institute of Scientific and Industrial Research, Osaka University. He stayed at ETH

Zurich as a visiting researcher in 2008 and moved to AIST in 2010. His primary research interests are computer vision, computer graphics and robotics (mainly geometrical modeling and visualization).



Yasuhiro Mukaigawa (M'03) received his M.E. and Ph.D. degrees from University of Tsukuba in 1994 and 1997, respectively. He became a research associate at Okayama University in 1997, an assistant professor at University of Tsukuba in 2003, and an associate professor at Osaka University in 2004. He joined the MIT Media Lab as a visiting associate professor from 2009 to 2010. He joined Nara Institute of Science and Technology in 2014 as a professor. His current research interests include computer vision and computational photography.



Yasushi Yagi (M'91) is the Director of the Institute of Scientific and Industrial Research, Osaka university, Ibaraki, Japan. He received his Ph.D. degrees from Osaka University in 1991. In 1985, he joined the Product Development Laboratory, Mitsubishi Electric Corporation, where he worked on robotics and inspections. He became a Research Associate in 1990, a Lecturer in 1993, an Associate Professor in 1996, and a Professor in 2003 at Osaka University. International conferences for which he has served as Chair include: FG1998 (Financial

Chair), OMINVIS2003 (Organizing chair), ROBIO2006 (Program co-chair), ACCV2007 (Program chair), PSVIT2009 (Financial chair), ICRA2009 (Technical Visit Chair), ACCV2009 (General chair), ACPR2011 (Program co-chair) and ACPR2013 (General chair). He has also served as the Editor of IEEE ICRA Conference Editorial Board (2007–2011). He is the Editorial member of IJCV and the Editor-in-Chief of IPSJ Transactions on Computer Vision & Applications. He was awarded ACM VRST2003 Honorable Mention Award, IEEE ROBIO2006 Finalist of T.J. Tan Best Paper in Robotics, IEEE ICRA2008 Finalist for Best Vision Paper, MIRU2008 Nagao Award, and PSIVT2010 Best Paper Award. His research interests are computer vision, medical engineering and robotics. He is a fellow of IPSJ and a member of IEICE and RSJ.